Analysis of the Influence of an XY Electronic Mechanism with UV-Vis Spectroscopy on the Production of Gold Nanoparticles by Laser Ablation for Applications in Environmental Nanosensing

Hipólito Carbajal-Morán[1*], Javier F. Márquez-Camarena[1], Ever F. Ingaruca-Álvarez[2], Rosa H. Zárate-Quiñones[3]

[1] Instituto de Investigación de Ciencias de Ingeniería, Facultad de Ingeniería Electrónica-Sistemas, Universidad Nacional de Huancavelica, Jr. La Mar 755, Pampas 09156, Huancavelica, Perú

[2] Facultad de Ingeniería Química, Universidad Nacional del Centro del Perú, Av. Mariscal Castilla N° 3909-4089, Huancayo 12006, Junín, Perú

[3] Facultad de Ciencias Forestales y del Ambiente, Universidad Nacional del Centro del Perú, Av. Mariscal Castilla N° 3909-4089, Huancayo 12006, Junín, Perú

* Corresponding author's e-mail: hipolito.carbajal@unh.edu.pe

ABSTRACT

The work consisted in analyzing the influence of an electronic positioning mechanism of an Au metal plate in the XY axes; to optimize the production of Au metal nanoparticles by laser ablation in sterile water samples as well as to obtain morphology and size required for environmental nanosensors. The positioning mechanism is constituted by two M35SP stepper motors of 5 V DC with a rotation angle of 7.5° per step; the one that generates the displacement for each axis of XY coordinates, controlled by an algorithm implemented in Arduino Nano ATmega328, being the driver of the stepper motors the H-bridge of the L298N module, with which it was possible to set the speed to 2 mm/s, which enabled to make the wear of the metal plate uniform in the process of generation of gold nanoparticles (AuNPs). With the pulsed laser generator with ablation frequency of 10 Hz and wavelengths of 532 nm and 1064 nm, the Au metal plate was irradiated for 10 min, 20 min and 30 min. AuNPs were generated in colloidal state both for the process with fixed position of the metal plate and for the process using the electronic mechanism of XY positioning; they were characterized by UV-Vis spectroscopy with range from 300 nm to 850 nm. It was found that the production of AuNPs with the Au plates mobilized by the mechanism under study, generates colloids of spherical AuNPs of smaller diameter, close to 10 nm, with an average reduction of 19% in relation to that generated with the fixed position plate; likewise, the concentration of the AuNPs increased by 20.40%; therefore, the influence of the XY positioning electronic mechanism was positive in the production of AuNPs with morphology and sizes suitable for use in environmental nanosensors.

Keywords: XY displacement, nanoparticles, step motor control, UV-Vis spectroscopy, nanosensor.

INTRODUCTION

The nanoparticles obtained from noble metals, especially AuNPs, exhibit excellent physical, chemical and biological properties, intrinsic to their nanometer size (Shih et al., 2020). Moreover, AuNPs can be produced in different sizes and shapes and can be applied in various fields of knowledge. This makes AuNPs of great interest in many areas, especially in the biomedical, food and environmental sectors (Dheyab et al., 2022; Paidari & Ibrahim, 2021).

The detection of polluting elements in the environment such as: air, soil and water require nanosensors of varied morphology, being able to be triangular, spherical among others; with wavelengths of absorption spectra close to 518 nm, which represents diameters of AuNPs close to 10 nm. The works that evidence a suitable morphology and size of AuNPs for environmental

applications include: Manjubaashini & Daniel Thangadurai (2023), who performed a review of naked eye detection of various metal ions using nanocomposites based on AuNPs; emphasizing the importance and applications of nanocomposite AuNPs in the detection of contaminant metal ions using a colorimetric approach as well as, their optical characteristics, synthesis techniques and future research objectives. Khani et al. (2022), developed a colorimetric assay for the detection of Hg_2^+ ions in real water samples based on a clock reaction catalyzed by 10 nm to 15 nm AuNPs; being a fast and naked eye detection process, which opens new ways for the generation of portable nanosensors applicable to the environment. Talan et al. (2018), developed an ultrasensitive electrochemical immunodetection platform based on fluorine-doped 10 nm AuNPs that activates the detection of chlorpyrifos in fruits and vegetables, due to its excellent stability, sensitivity and simplicity. Anwar et al. (2018), synthesized AuNPs with diameter close to 10 nm, stabilizing with a ligand, obtaining a colorimetric nanosensor for the detection of heavy metal Pd (II) in water.

The size of nanoparticles are related to the resonance length of Au plasmon resonance; a length near 518 nm corresponds to AuNPs with diameter of 10 nm and a length near 520 nm corresponds to AuNPs with diameter of 20 nm with spherical shape and distinctive color of red-colored colloidal suspensions (Herbani et al., 2018; Shin et al., 2022). Obtaining uniform-sized nanoparticles by laser ablation and other methods is relatively complicated; for nanoparticle synthesis, there are mainly chemical and physical approaches. In particular, in nanoparticle synthesis, it is admitted that the physical approach should be complemented with the classical chemical one in the doping process. The former seems more preferable than the latter because the chemical one involves various kinds of toxic chemicals which are difficult to clean up afterwards (Qayyum et al., 2019).

Of the available physical approaches pulsed laser ablation in liquid (PLAL) is one of the most acceptable as it does not contain dissolved chemical contaminants (Gentile et al., 2021); likewise, production of AuNPs with a uniform distribution is possible depending on mechanisms and strategies adopted for their production and a relatively uniform distribution of nanoparticles can be generated (Herbani et al., 2018). In this PLAL approach it is necessary, among the various parameters, to have a mechanism that allows keeping in motion the solid metallic gold plate that is the target, to improve the obtaining of metallic nanoparticles by fragmentation of the material immersed in sterile water (Naser et al., 2021), yielding nanometric material in colloidal state with interesting properties applicable to various research areas, such as the detection of heavy metals in water (Carbajal-Morán et al., 2022), as in environmental applications in general.

Regarding displacement mechanisms, there are several studies where positioners in the XY plane were designed. Shi et al. (2015), designed an XY nanopositioner for parallel kinematic microelectromechanical systems (MEMS), used for decoupled motions, this mechanism has three parts: actuator, displacement amplifier and guiding mechanism; this nanopositioner can travel 83×83 µm. Likewise, Liao et al. (2022), implemented an open source and low-cost XYZ nanopositioner for high-precision analytical applications with payload capacity up to 12 kg; moreover, it does not require adjustments, being able to have practical applications in measurements, such as microscopy.

Also, Guver et al. (2019), built an XY micromanipulator using stepper motors, an Arduino Nano controller, with couplers and gears for the motorized stage; the control of the motors was performed employing open-source software. Mucciaroni & Vivas (2021), configured a homemade optical microscope with a 3D translation stage using low-cost stepper motors and controlled by Arduino, the setup was able to perform XY translational motion with travel range of 25 mm and scanning speeds up to 1.35 mm/s. Romero et al. (2019), developed a computerized system for sample displacement with stepper motor using the L298, avoiding the use of a traditional complex electronic circuit of multiple discrete components, using a bipolar stepper motor with coupling to the translation stage for Z scanning where precise displacement of the samples is required; the myDAQ device was used, with an easy to use interface in LabVIEW.

The XY displacement mechanism can be achieved with electronic control elements constituted by Arduino Nano which is one of the development boards based on ATmega328P microcontroller and usable even in Internet of Things (Kurniawan, 2021), the microcontroller of Arduino Nano is programmable in Arduino IDE. Bipolar stepper motors are easy to control, each turn is called a step, the most common step angles are

30°, 15°, 7.5°, 5°, 2.5° and 1.8°; the smaller the step, the better the resolution (Hao et al., 2022). The fundamental element for power control of DC motors and stepper motors is an H-bridge configured in the L298N module (Virgala et al., 2015).

Therefore, in order to improve the production of AuNPs in colloidal state with the PLAL approach for applications in environmental nanosensors, the work aimed to evaluate an electronic mechanism implemented for the displacement with stepper motors of the Au metal plate in the XY plane and the improvement of the morphology, diameter and concentration in the production of AuNPs by laser ablation in sterile water samples of pH 6.92 and conductivity ≤ 1 µS/cm.

MATERIALS AND METHODS

In the construction of the XY positioner an Arduino Nano ATmega328P was used; the displacement was generated by the M35SP stepper motors of 5 V DC with rotation angle of 7.5° per step, for each coordinate axis, so 48 steps were necessary for a complete turn; the power control of the motors was performed by means of the H-bridge configured in the L298N driver module. The required structure for any XY positioner must be light and therefore aluminum was used. A practical and simple way to perform the X or Y displacement is by using two mechanisms, mounted one on top of the other, one corresponding to the X coordinate and the other to Y (see Figure 1).

Likewise, stops were necessary at each end of the slides using limit switches for both the X and Y axes, which allowed the initial positioning (0.0) to place the Au metal plate in 20 ml of water and the space to be limited to an area of 150 mm², which is the size of the Au metal plate (see Figure 2). The stepper motors (Motor1 and Motor2) were bipolar 4-phase MP35SP with working voltage of 5 V DC, coil resistance of 50 ohm, with step angle of 7.5°, torque 23 mN/200 pps, with current consumption less than 259 mA, so the peak power dissipated was less than 1,280 W.

The algorithm for stepper motor displacement control for both X-axis and Y-axis positioning is presented in Figure 3; this algorithm was
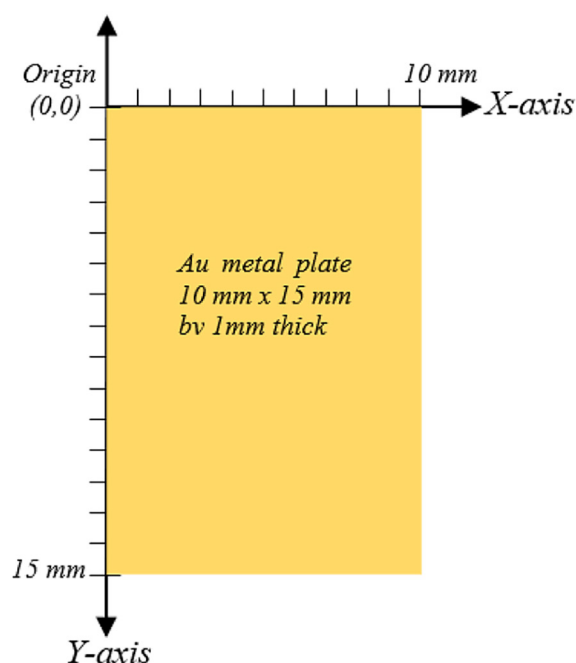
Figure 2. XY coordinates to generate AuNPs
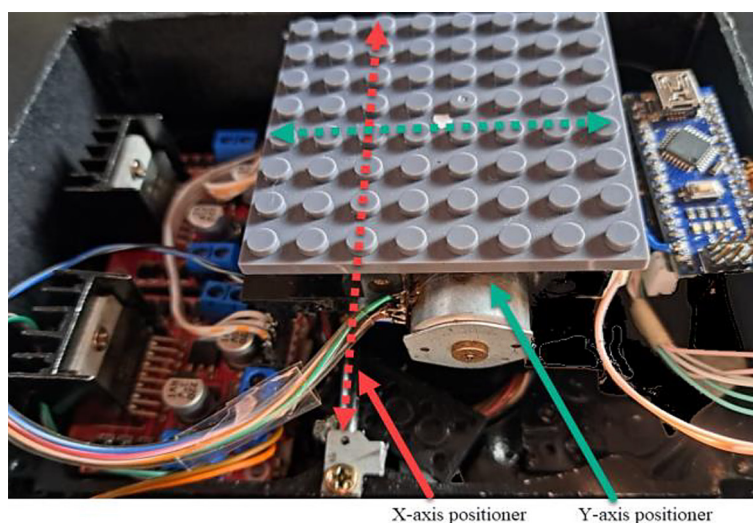
Figure 1. XY positioning mechanism
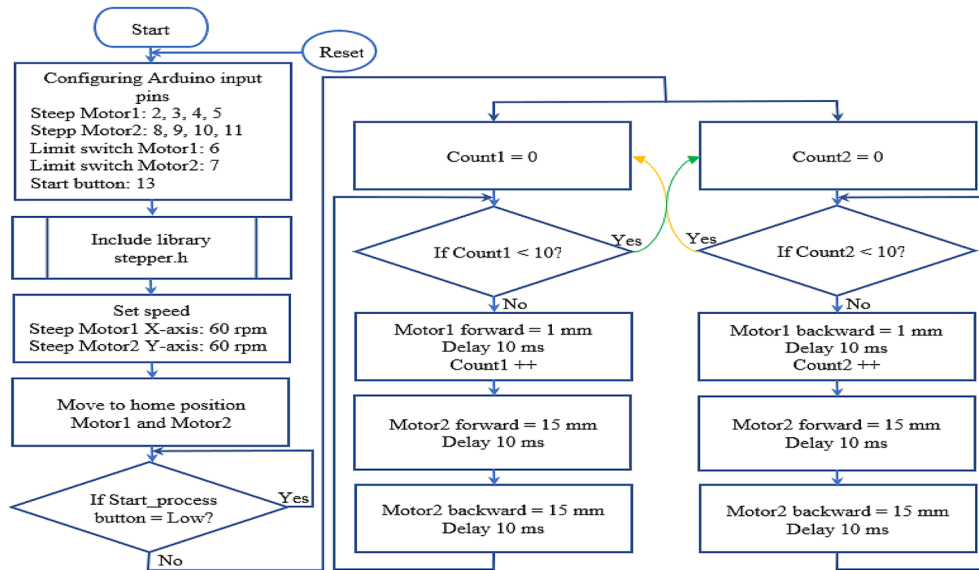
Figure 3. Step-by-step motor control algorithm for XY positioning of the Au metal plate

implemented on Arduino Nano ATmega328P and programmed from Arduino IDE 2.4. 0 (Arduino, 2022), the control process starts with the configuration of the Arduino pins, then a special library (stepper.h) for stepper motor control is included, the speed of the motors is set and then positioned at the XY origin (0,0); pressing "Start_process" starts with the positioning of the Au metal sample contained in sterile water. At first, Motor1 advances 1 mm forward; then Motor2 advances 15 mm forward along the Y axis, then returns 15 mm, and then repeats this sequence until Motor1 reaches 10 mm of travel; then Motor1 returns step by step with an advance of 1 mm backward while Motor2 continues with the cyclic sequence of advancing 15 mm forward and 15 mm backward. Once positioned again at the origin (0,0) the sequence is repeated indefinitely until the "Reset" button is activated, which allows starting the whole process again in the controller. To start with the operation of the mechanism implemented according to the electronic control circuit diagram in Figure 4, it is
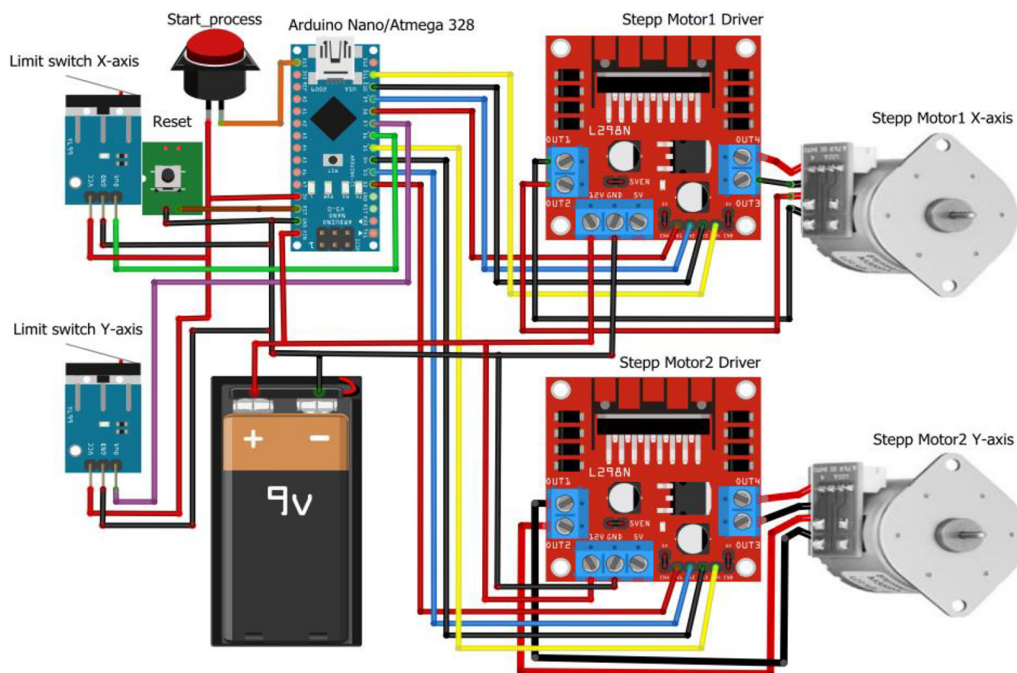
Figure 4. Diagram of the electronic control circuit of the stepper motors for XY positioning of the Au metal plate

powered with a 9 V DC battery; both the Arduino Nano and the L298N driver modules to control the bipolar stepper motors; the limit switches of the XY axes and the "Start_process" button are powered with 5 V DC which is generated by the LM117 voltage regulator located in the Arduino Nano.

For the production of AuNPs, the pulsed Nd:Yag laser equipment offered by Quantel, Q-Smart 450 series was used; this equipment is compact with high performance and energy stability, and with low divergence output beam. Its applications include: spectroscopy, flash photolysis and laser ablation which is used in this work (Quantel, 2019). It was configured for a laser pulse rate of 2 Hz; both for wavelength 1064 nm with energy ≥ 450 mJ/p, and for wavelength 532 nm employing the frequency doubler module (2ω), being the energy ≥220 mJ/p (see Figure 5); with which AuNPs were produced for periods of 10 min, 20 min and 30 min with a pulsed laser duration of 116 μs, for all cases.

The generated AuNPs were characterized with the Avantes UV-Vis spectroscope with wavelength 200–1160 nm; the light for the sensor is generated by deuterium and halogen lamps with wavelength 200–1700 nm. The sensor samples up to 64-bit values; thus, it covers signals in the ultraviolet and infrared range. The measurement is performed via FC/PC fiber optic connectors; with Avantes (2018) AvaSoft software for PC, the signals are sampled every 2 milliseconds. In line with Figure 6, the sequence for the characterization of the samples starts with the immersion of the photodiode sensor in the AuNPs colloid, then they are interpreted by the spectrometer and sent to the AvaSoft software interface where the ratio of the absorption spectra (A.U) and their respective wavelength (nm) is defined graphically; with
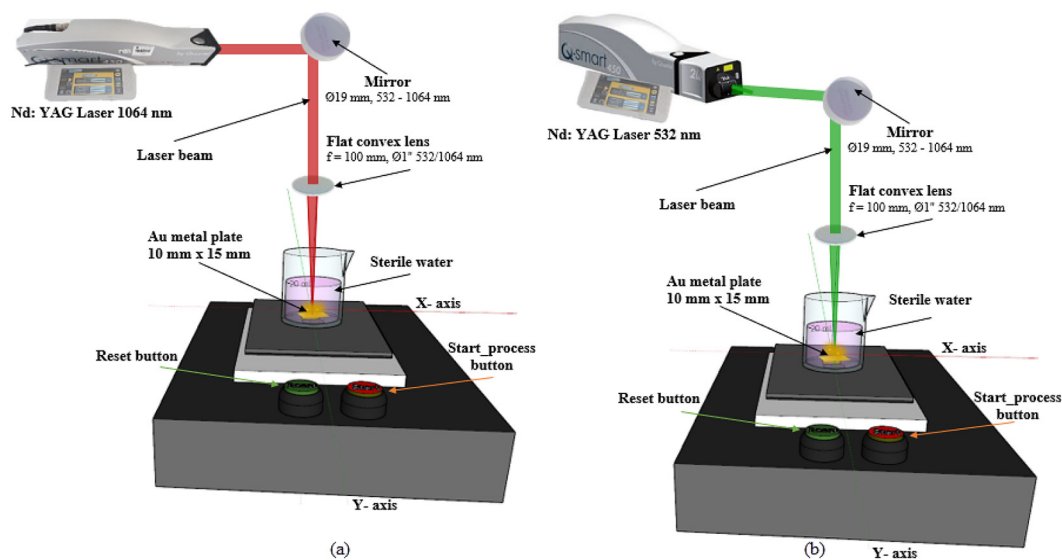
Figure 5. Installation of the laser equipment with the electronic XY positioning mechanism to produce AuNPs (a) with 1064 nm laser and (b) with 532 nm laser
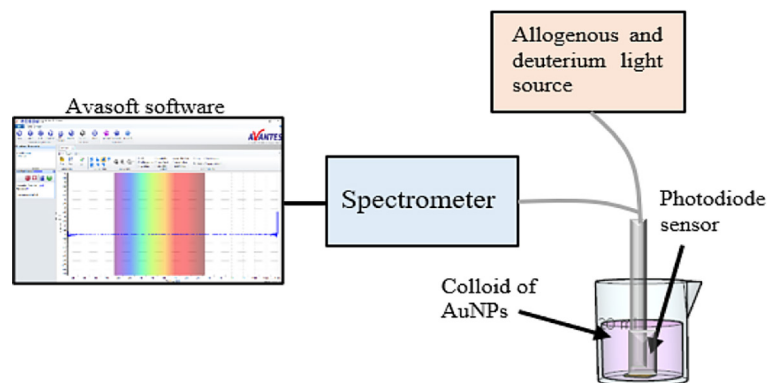
Figure 6. Diagram for characterization of AuNPs colloids

which it is possible to determine the diameter and concentration of the AuNPs.

With the wavelength values of the spectrum and the absorbance, the diameters of the AuNPs were calculated; using Equation 1 (Haiss et al., 2007),

$$d = \frac{\ln\left(\frac{\lambda_{spr}-512}{6.530}\right)}{0.0216} \qquad (1)$$

where: λ_{spr} – the absorbance of the AuNPs.

Likewise, the concentration of AuNPs (c_{Au}) was calculated using Equation 2.

$$d = \left(\frac{A_{spr}(5.89 * 10^{-6})}{c_{Au} * exp(-4.75)}\right)^{1/0.314} \qquad (2)$$

where: A_{spr} – represents the peak absorbance of AuNPs.

RESULTS AND DISCUSSION

By irradiating the gold metal plate with fixed position, using the Q-Smart 450 laser equipment, nanoparticles were produced by the effect of pulsed laser ablation. At first, laser pulses were irradiated with a delay of 116 µs and wavelength of 1064 nm with approximate power of 450 mJ/p; for 10 min, 20 min and 30 min, obtaining signals with absorption spectra of 0.16 A.U., 0.33 A.U. and 0.51 A.U. respectively; likewise, the wavelengths were 523.13 nm, 521.37 nm and 520.19 nm which corresponds to the laser irradiation time (see Figure 7a). Then, laser pulses were irradiated with a delay of 116 µs and wavelength of 532 nm with power of approximately 220 mJ/p; for 10 min, 20 min and 30 min, obtaining signals with absorption spectra of 0.07 A.U., 0.29 A.U. and 0.44 A.U. respectively; likewise, the wavelengths were 523.72 nm, 523.13 nm and 521.95 nm which corresponds to the laser irradiation time (see Figure 7b).

Table 1 presents the diameter and colloid concentration of AuNPs calculated with Equations 1 and 2, based on the absorbance and peak wavelength presented in Figures 7a and 7b; the obtained diameter of AuNPs decreases with longer laser irradiation, both for the 532 nm laser (27.08–19.50 nm), as well as for the 1064 nm laser (24.69–10.43 nm); in turn, the colloid concentration of AuNPs increases (0.169– 1.663 µg/ml) as time passes, due to post-irradiation. When using the electronic mechanism of XY positioning for displacement of the Au metal plate submerged in sterile water, in the XY plane, with the same Q-Smart 450 laser equipment and by pulsed laser ablation, with a delay of 116 µs and wavelength of 1064 nm with approximate power of 450 mJ/p, for 10 min, 20 min and 30 min, signals were obtained with absorption spectra of 0.16 A.U., 0.36 A.U. and 0.55 A.U. respectively, 0.36 A.U. and 0.55 A.U. respectively. Likewise, the wavelengths were 523.13 nm, 520.78 nm and 520.18 nm, corresponding to the laser irradiation time (see Figure 8a). When irradiating laser pulses with delay 116 µs and wavelength 532 nm with approximate power of 220 mJ/p, for 10 min, 20 min and 30 min, signals with absorption spectra of 0.09 A.U., 0.32 A.U. and 0.52 A.U. respectively, were obtained, being the wavelengths 522.54 nm,
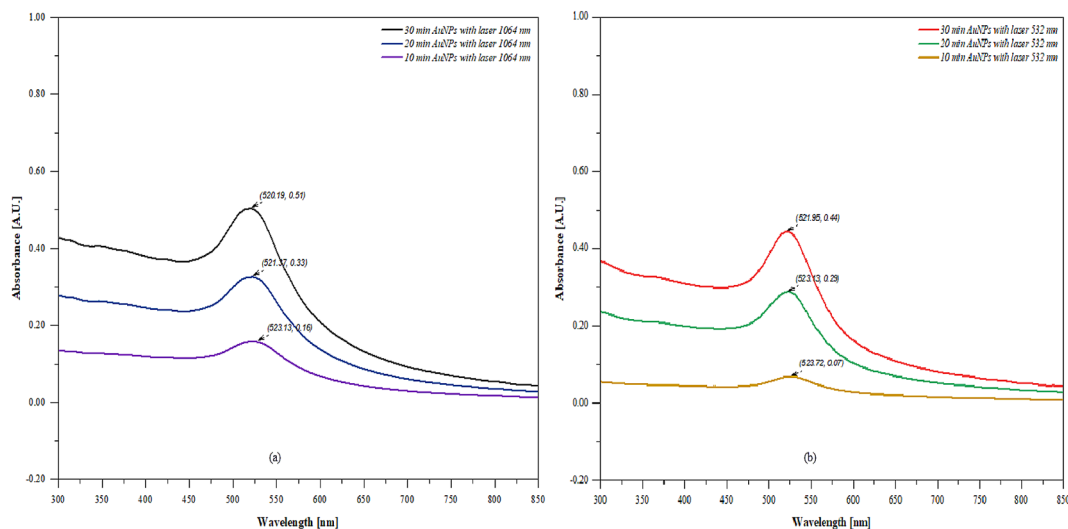
Figure 7. Absorbance spectra of AuNPs colloids produced with fixed metal plate by laser ablation; (a) 1064 nm and (b) 532 nm

521.37 nm and 520.19 nm which is related to the laser irradiation time (see Figure 8b).

Table 2 presents the diameter and colloid concentration of AuNPs calculated also with Equations 1 and 2, based on the absorbance and peak wavelength presented in Figures 8a and 8b. The obtained diameter of AuNPs decreases as it is irradiated with laser for longer time, both for the 532 nm laser (22.17– 10.49 nm), as well as for the 1064 nm laser (24.69–10.43 nm); in turn, the colloid concentration of AuNPs increases (0.230–1.826 µg/ml) as time passes, due to post-irradiation.

Table 3 is obtained from Tables 1 and 2, where the differences in the diameter and concentration of AuNPs colloids obtained with Au metal plate in fixed position and Au metal plate in movement generated by the XY positioning electronic mechanism are presented; this difference was calculated from Figures 7 and 8, subtracting the wavelength and absorbance values

Table 1. Diameter and concentration of AuNPs colloids obtained with fixed Au metal plate

Water sample parameters	Laser wavelength	Time	Peak absorbance	Peak wavelength	Diameter	Concentration
	(nm)	(min)	(A.U.)	(nm)	(nm)	(µg/ml)
pH = 6.92 Conductivity ≤ 1 uS/cm	532 (≥ 220mJ)	10	0.07	523.72	27.08	0.169
		20	0.29	523.13	24.69	0.721
		30	0.44	521.95	19.50	1.179
	1064 (≥ 450 mJ)	10	0.16	523.13	24.69	0.398
		20	0.33	521.37	16.72	0.928
		30	0.51	520.18	10.43	1.663
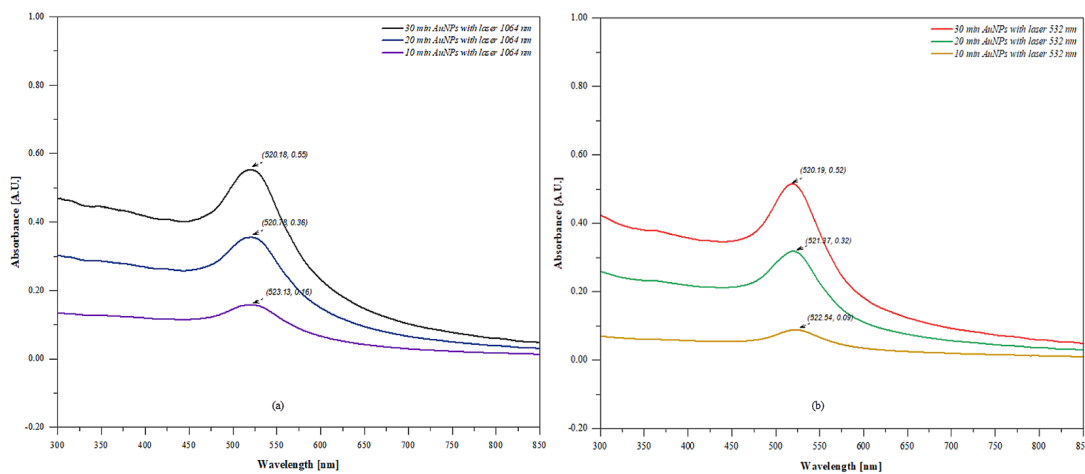
Figure 8. Absorbance spectra of AuNPs colloids produced by laser ablation with Au metal plate moving through the XY electronic positioning mechanism; (a) at 1064 nm and (b) at 532 nm

Table 2. Diameter and concentration of AuNPs colloids obtained with Au metal plate positioned by XY electronic displacement mechanism

Water sample parameters	Laser wavelength	Time	Peak absorbance	Peak wavelength	Diameter	Concentration
	(nm)	(min)	(A.U.)	(nm)	(nm)	(µg/ml)
pH = 6.92 Conductivity ≤ 1 uS/cm	532 (≥ 450 mJ)	10	0.09	522.54	22.17	0.230
		20	0.32	521.37	16.72	0.900
		30	0.52	520.19	10.49	1.693
	1064 (≥ 220 mJ)	10	0.16	523.13	24.69	0.398
		20	0.36	520.78	13.71	1.077
		30	0.56	520.18	10.43	1.826

Table 3. Difference in diameter and concentration of AuNPs colloids obtained with fixed Au metal plate and Au metal plate positioned by the XY electronic displacement mechanism

Water sample parameters	Laser wavelength	Time	Peak absorbance difference	Peak wavelength difference	Diameter difference	Concentration difference
	(nm)	(min)	(A.U.)	(nm)	(nm)	(µg/ml)
pH = 6.92 Conductivity ≤ 1 uS/cm	532 (≥ 450 mJ)	10	0.02	-1.18	-4.91	0.062
		20	0.03	-1.76	-7.97	0.178
		30	0.08	-1.76	-9.01	0.514
	1064 (≥ 220 mJ)	10	0.00	0.00	0.00	0.000
		20	0.03	-0.59	-3.01	0.149
		30	0.05	0.00	0.00	0.019

found when characterizing by UV–Vis spectroscopy. It is evidenced that the AuNPs colloids generated by 1064 nm and 532 nm laser with Au metal plate in fixed position immersed in 20 ml of sterile water of pH = 6.92 and conductivity ≤ 1 µS/cm, have a larger diameter and lower concentration; while the AuNPs colloids generated by the same 1064 nm and 532 nm laser equipment with Au metal plate in motion by action of the XY positioning mechanism, also immersed in 20 ml of sterile water, with the same parameters as the previous one, have a smaller diameter and higher concentration.

From the results found, it can be affirmed that the electronic mechanism of XY positioning with respect to Au plates in fixed position, positively influences the generation of AuNPs colloids due to the effects of post-irradiation uniformized by this mechanism both in the wear of the Au metal plate and in the generated colloid, obtaining spherical AuNPs with a diameter of approximately 10.41 nm, which would be suitable for use in applications with environmental nanosensors.

CONCLUSIONS

The electronic mechanism of XY positioning was implemented, the control of which was performed from Arduino Nano with ATmega328P processor driven by the H–bridge of the L298N driver module for the stepper motors of 7.5° being necessary 48 steps for a complete turn; the configuration for the X or Y displacement was to use two mechanisms mounted one on top of the other one corresponds to the X axis and the one on top corresponds to the Y axis. It presented a displacement speed of 2 mm/s, able to displace the whole surface

of the Au metal plate of dimensions 10×15 mm with a thickness of 1 mm in 155 s. AuNPs colloids were generated using the Q-Smart 450 laser equipment, both with the Au metal plate in fixed position and with the metal plate positioned by the XY electronic mechanism; both immersed in sterile water with pH = 6.92 and conductivity ≤ 1 µS/cm. AuNPs were produced by laser ablation at a focal distance of 30 cm, with a delay of 116 µs and wavelengths of 1064 nm and 532 nm with approximate power of 450 mJ/p and 220 mJ/p respectively for periods of 10 min, 20 min and 30 min.

By performing the analysis by UV-Vis spectroscopy to the AuNPs colloids produced by the same laser equipment of 1064 nm and 532 nm, both with the Au metal plate in fixed position, and with the Au metal plate moving by action of the XY positioning mechanism, immersed in 20 ml of sterile water of pH = 6.92 and conductivity ≤ 1 µS/cm, it was found that the production of AuNPs with the Au plates mobilized by the mechanism under study generates AuNPs of smaller diameter with an average reduction of 19% with respect to that generated with the fixed position plate. Likewise, the concentration of the AuNPs was higher increasing by 20.40%; therefore, the influence of the XY positioning electronic mechanism was positive in the production of AuNPs in sterile water samples. Due to the morphology and dimensions close to 10 nm, they are suitable for use in environmental nanosensors.

REFERENCES

1. Anwar, A., Minhaz, A., Khan, N.A., Kalantari, K., Afifi, A.B.M., Shah, M.R. 2018. Synthesis of gold nanoparticles stabilized by a pyrazinium thioacetate ligand: A new colorimetric nanosensor for detection of heavy metal Pd(II). Sensors and Actuators B: Chemical, 257, 875–881. https://doi.org/https://doi.org/10.1016/j.snb.2017.11.040

2. Arduino. 2022. Software Arduino IDE. https://www.arduino.cc/en/software

3. Avantes. 2018. Espectrómetro UV-Vis-NIR - AvaSpec-ULS2048x64-EVO. https://www.medicalexpo.com/prod/avantes/product-104219-950813.html

4. Carbajal-Morán, H., Rivera-Esteban, J.M., Aldama-Reyna, C.W., Mejía-Uriarte, E.V. 2022. Functionalization of Gold Nanoparticles for the Detection of Heavy Metals in Contaminated Water Samples in the Province of Tayacaja. Journal of Ecological Engineering, 23(9), 88–99. https://doi.org/10.12911/22998993/151745

5. Dheyab, M.A., Aziz, A.A., Moradi Khaniabadi, P., Jameel, M.S., Oladzadabbasabadi, N., Mohammed, S.A., Abdullah, R.S., Mehrdel, B. 2022. Monodisperse gold nanoparticles: A review on synthesis and their application in modern medicine. International Journal of Molecular Sciences, 23(13), 7400.

6. Gentile, L., Mateos, H., Mallardi, A., Dell'Aglio, M., De Giacomo, A., Cioffi, N., Palazzo, G. 2021. Gold nanoparticles obtained by ns-pulsed laser ablation in liquids (ns-PLAL) are arranged in the form of fractal clusters. Journal of Nanoparticle Research, 23(2), 35.

7. Guver, A., Fifita, N., Milas, P., Straker, M., Guy, M., Green, K., Yildirim, T., Unlu, I., Yigit, M.V., Ozturk, B. 2019. A low-cost and high-precision scanning electrochemical microscope built with open source tools. HardwareX, 6, e00082. https://doi.org/https://doi.org/10.1016/j.ohx.2019.e00082

8. Haiss, W., Thanh, N.T.K., Aveyard, J., Fernig, D.G. 2007. Determination of size and concentration of gold nanoparticles from UV− Vis spectra. Analytical Chemistry, 79(11), 4215–4221.

9. Hao, X., Xia, G., Zhang, S., Zhou, Z., Du, M., Ding, X. 2022. Study of metal 3D printing stepper motor control based on S-trapezoid algorithm. 2022 5th World Conference on Mechanical Engineering and Intelligent Manufacturing (WCMEIM), 1107–1111.

10. Herbani, Y., Irmaniar, Nasution, R.S., Mujtahid, F., Masse, S. 2018. Pulse laser ablation of Au, Ag, and Cu metal targets in liquid for nanoparticle production. Journal of Physics: Conference Series, 985(1), 12005. https://doi.org/10.1088/1742-6596/985/1/012005

11. Khani, H., Abbasi, S., Tavakkoli Yaraki, M., Tan, Y.N. 2022. A naked-eye colorimetric assay for detection of Hg2+ ions in real water samples based on gold nanoparticles-catalyzed clock reaction. Journal of Molecular Liquids, 345, 118243. https://doi.org/https://doi.org/10.1016/j.molliq.2021.118243

12. Kurniawan, A. 2021. Iot projects with arduino nano 33 ble sense. Berkeley: Apress, 129.

13. Liao, H.-S., Werner, C., Slipets, R., Emil Larsen, P., Hwang, I.-S., Chang, T.-J., Ulrich Danzebrink, H., Huang, K.-Y., Hwu, E.-T. 2022. Low-cost, open-source XYZ nanopositioner for high-precision analytical applications. HardwareX, 11, e00317. https://doi.org/https://doi.org/10.1016/j.ohx.2022.e00317

14. Manjubaashini, N., Daniel Thangadurai, T. 2023. Unaided-eye detection of diverse metal ions by AuNPs-based nanocomposites: A review. Microchemical Journal, 190, 108628. https://doi.org/https://doi.org/10.1016/j.microc.2023.108628

15. Mucciaroni, L.R., Vivas, M.G. 2021. Efficient Yet Accessible Arduino-based Control System for Laser Microfabrication of Photonic Platforms. Lasers in Manufacturing and Materials Processing, 8(4), 395–408. https://doi.org/10.1007/s40516-021-00153-3

16. Naser, H., Shanshool, H.M., Imhan, K.I. 2021. Parameters Affecting the Size of Gold Nanoparticles Prepared by Pulsed Laser Ablation in Liquid. Brazilian Journal of Physics, 51(3), 878–898. https://doi.org/10.1007/s13538-021-00875-x

17. Paidari, S., Ibrahim, S.A. 2021. Potential application of gold nanoparticles in food packaging: a mini review. Gold Bulletin, 54, 31–36.

18. Qayyum, H., Ali, R., Rehman, Z.U., Ullah, S., Shafique, B., Dogar, A.H., Shah, A., Qayyum, A. 2019. Synthesis of silver and gold nanoparticles by pulsed laser ablation for nanoparticle enhanced laser-induced breakdown spectroscopy. Journal of Laser Applications, 31(2), 22014.

19. Quantel. 2019. Q-smart 450 Pulsed Nd:YAG Laser, 213 to 1064nm, 8 to 450mJ, Product - Photonic Solutions, UK. https://www.photonicsolutions.co.uk/product-detail.php?prod=6345

20. Romero, A.L.S., Barbano, E.C., Misoguti, L. 2019. Computerized system for sample displacement with stepper motor using the L298: application in the Z-scan technique. Revista Brasileira de Ensino de Física, 41. https://doi.org/10.1590/1806-9126-RBEF-2019-0018

21. Shi, H., Kim, Y., She, Y. 2015. Design of a parallel kinematic MEMS XY nanopositioner. 2015 IEEE International Conference on Robotics and Biomimetics (ROBIO), 1973–1978. https://doi.org/10.1109/ROBIO.2015.7419062

22. Shih, C.-Y., Shugaev, M.V, Wu, C., Zhigilei, L.V. 2020. The effect of pulse duration on nanoparticle generation in pulsed laser ablation in liquids: insights from large-scale atomistic simulations. Physical

Chemistry Chemical Physics, 22(13), 7077–7099.

23. Shin, M., Yang, S., Kwak, H.W., Lee, K.H. 2022. Synthesis of gold nanoparticles using silk sericin as a green reducing and capping agent. European Polymer Journal, 164, 110960. https://doi.org/https://doi.org/10.1016/j.eurpolymj.2021.110960

24. Talan, A., Mishra, A., Eremin, S.A., Narang, J., Kumar, A., Gandhi, S. 2018. Ultrasensitive electrochemical immuno-sensing platform based on gold nanoparticles triggering chlorpyrifos detection in fruits and vegetables. Biosensors and Bioelectronics, 105, 14–21. https://doi.org/https://doi.org/10.1016/j.bios.2018.01.013

25. Virgala, I., Kelemen, M., Gmiterko, A., Lipták, T. 2015. Control of stepper motor by microcontroller. Journal of Automation and Control, 3(3), 131–134.